HHS Public Access

Author manuscript

ACS Nano. Author manuscript; available in PMC 2023 December 22.

Published in final edited form as:

ACS Nano. 2022 November 22; 16(11): 18223–18231. doi:10.1021/acsnano.2c05687.

Microneedle Patches Loaded with Nanovesicles for Glucose Transporter-Mediated Insulin Delivery

Qian Chen[●],

Department of Bioengineering, University of California, Los Angeles, California 90095, United States

California NanoSystems Institute, University of California, Los Angeles, California 90095, United States

Joint Department of Biomedical Engineering, University of North Carolina at Chapel Hill and North Carolina State University, Raleigh, North Carolina 27695, United States

Institute of Functional Nano & Soft Materials (FUNSOM), Jiangsu Key Laboratory for Carbon-Based Functional Materials & Devices, Soochow University, Suzhou 215123

Zhisheng Xiao[●],

Institute of Functional Nano & Soft Materials (FUNSOM), Jiangsu Key Laboratory for Carbon-Based Functional Materials & Devices, Soochow University, Suzhou 215123, China

Chao Wang[●],

Joint Department of Biomedical Engineering, University of North Carolina at Chapel Hill and North Carolina State University, Raleigh, North Carolina 27695, United States

Corresponding Authors: Qian Chen – Department of Bioengineering, University of California, Los Angeles, California 90095, United States; California NanoSystems Institute, University of California, Los Angeles, California 90095, United States; Joint Department of Biomedical Engineering, University of North Carolina at Chapel Hill and North Carolina State University, Raleigh, North Carolina 27695, United States; Institute of Functional Nano & Soft Materials (FUNSOM), Jiangsu Key Laboratory for Carbon-Based Functional Materials & Devices, Soochow University, Suzhou 215123, China; chenqian@suda.edu.cn, **Xiao Ye** – Geriatric Medicine Center, Department of Endocrinology, Zhejiang Provincial People's Hospital (Affiliated People's Hospital, Hangzhou Medical College), Hangzhou, Zhejiang 310014, China; Key Laboratory for Diagnosis and Treatment of Endocrine Gland Diseases of Zhejiang Province, Hangzhou, Zhejiang 310014, China; semper_fi@foxmail.com, **Zhen Gu** – Department of Bioengineering, University of California, Los Angeles, California 90095, United States; California NanoSystems Institute, University of California, Los Angeles, California 90095, United States; Joint Department of Biomedical Engineering, University of North Carolina at Chapel Hill and North Carolina State University, Raleigh, North Carolina 27695, United States; Key Laboratory of Advanced Drug Delivery Systems of Zhejiang Province, College of Pharmaceutical Sciences, Zhejiang University, Hangzhou 310058, China; Jinhua Institute of Zhejiang University, Jinhua 321299, China; Department of General Surgery, Sir Run Run Shaw Hospital, School of Medicine, Zhejiang University, Hangzhou 310016, China; Zhejiang Laboratory of Systems & Precision Medicine, Zhejiang University Medical Center, Hangzhou 311121, China; MOE Key Laboratory of Macromolecular Synthesis and Functionalization, Department of Polymer Science and Engineering, Zhejiang University, Hangzhou 310027, China; guzhen@ucla.edu.

●Author Contributions

Q.C., Z.X., and C.W. contributed equally to this study.

The authors declare the following competing financial interest(s): Z.G. and Q.C. have applied for patents related to this study. Z.G. is a scientific cofounder of ZenCapsule Inc., Zcapsule Inc., Zenomics Inc., and Wskin Inc. M.R.P. has a financial interest in microneedle patch technologies; the associated conflict of interest is managed by Georgia Tech.

ASSOCIATED CONTENT

Supporting Information

The Supporting Information is available free of charge at https://pubs.acs.org/doi/10.1021/acsnano.2c05687.

Discussions of experimental methods and figures of immunofluorescence imaging of GLUT4 in RBC vesicles, MALDI MS assay of glucose-insulin conjugates, SDS–PAGE analysis of purified GLUT1, confocal microscopy images of Glu-insulin-attached liposome-GLUT1, representative fluorescence images of skin, and *in vitro* accumulated liposome release from the microneedle (PDF)

Complete contact information is available at: https://pubs.acs.org/10.1021/acsnano.2c05687

Institute of Functional Nano & Soft Materials (FUNSOM), Jiangsu Key Laboratory for Carbon-Based Functional Materials & Devices, Soochow University, Suzhou 215123, China

Guojun Chen,
Department of Bioengineering, University of California, Los Angeles, California 90095, United States

California NanoSystems Institute, University of California, Los Angeles, California 90095, United States

Joint Department of Biomedical Engineering, University of North Carolina at Chapel Hill and North Carolina State University, Raleigh, North Carolina 27695, United States

Yuqi Zhang,
Department of Bioengineering, University of California, Los Angeles, California 90095, United States

California NanoSystems Institute, University of California, Los Angeles, California 90095, United States

Joint Department of Biomedical Engineering, University of North Carolina at Chapel Hill and North Carolina State University, Raleigh, North Carolina 27695, United States

Key Laboratory of Advanced Drug Delivery Systems of Zhejiang Province, College of Pharmaceutical Sciences, Zhejiang University, Hangzhou 310058, China

Xudong Zhang,
Department of Bioengineering, University of California, Los Angeles, California 90095, United States

California NanoSystems Institute, University of California, Los Angeles, California 90095, United States

Joint Department of Biomedical Engineering, University of North Carolina at Chapel Hill and North Carolina State University, Raleigh, North Carolina 27695, United States

Xiao Han,
Department of Bioengineering, University of California, Los Angeles, California 90095, United States

California NanoSystems Institute, University of California, Los Angeles, California 90095, United States

Jinqiang Wang,
Department of Bioengineering, University of California, Los Angeles, California 90095, United States

California NanoSystems Institute, University of California, Los Angeles, California 90095, United States

Joint Department of Biomedical Engineering, University of North Carolina at Chapel Hill and North Carolina State University, Raleigh, North Carolina 27695, United States

Key Laboratory of Advanced Drug Delivery Systems of Zhejiang Province, College of Pharmaceutical Sciences, Zhejiang University, Hangzhou 310058, China

Xiao Ye,
Geriatric Medicine Center, Department of Endocrinology, Zhejiang Provincial People's Hospital (Affiliated People's Hospital, Hangzhou Medical College), Hangzhou, Zhejiang 310014, China

Key Laboratory for Diagnosis and Treatment of Endocrine Gland Diseases of Zhejiang Province, Hangzhou, Zhejiang 310014, China

Mark R. Prausnitz,
School of Chemical and Biomolecular Engineering, Georgia Institute of Technology, Atlanta, Georgia 30332, United States

Song Li,
Department of Bioengineering, University of California, Los Angeles, California 90095, United States

California NanoSystems Institute, University of California, Los Angeles, California 90095, United States

Zhen Gu
Department of Bioengineering, University of California, Los Angeles, California 90095, United States

California NanoSystems Institute, University of California, Los Angeles, California 90095, United States

Joint Department of Biomedical Engineering, University of North Carolina at Chapel Hill and North Carolina State University, Raleigh, North Carolina 27695, United States

Key Laboratory of Advanced Drug Delivery Systems of Zhejiang Province, College of Pharmaceutical Sciences, Zhejiang University, Hangzhou 310058, China

Jinhua Institute of Zhejiang University, Jinhua 321299, China

Department of General Surgery, Sir Run Run Shaw Hospital, School of Medicine, Zhejiang University, Hangzhou 310016, China

Zhejiang Laboratory of Systems & Precision Medicine, Zhejiang University Medical Center, Hangzhou 311121, China

MOE Key Laboratory of Macromolecular Synthesis and Functionalization, Department of Polymer Science and Engineering, Zhejiang University, Hangzhou 310027, China

Abstract

Glucose-responsive insulin delivery systems that mimic insulin secretion activity in the pancreas show great potential to improve clinical therapeutic outcomes for people with type 1 and advanced type 2 diabetes. Here, we report a glucose-responsive insulin delivery microneedle (MN) array patch that is loaded with red blood cell (RBC) vesicles or liposome nanoparticles containing glucose transporters (GLUTs) bound with glucosamine-modified insulin (Glu-Insulin). In hyperglycemic conditions, high concentrations of glucose in interstitial fluid can replace

Glu-Insulin *via* a competitive interaction with GLUT, leading to a quick release of Glu-Insulin and subsequent regulation of blood glucose (BG) levels *in vivo*. To prolong the effective glucose-responsive insulin release from MNs, additional free Glu-Insulin, which serves as "stored insulin", is loaded after RBC vesicles or liposome nanoparticles bound with Glu-Insulin. In the streptozotocin (STZ)-induced type 1 diabetic mouse model, this smart GLUT-based insulin patch can effectively control BG levels without causing hypoglycemia.

Graphical Abstract

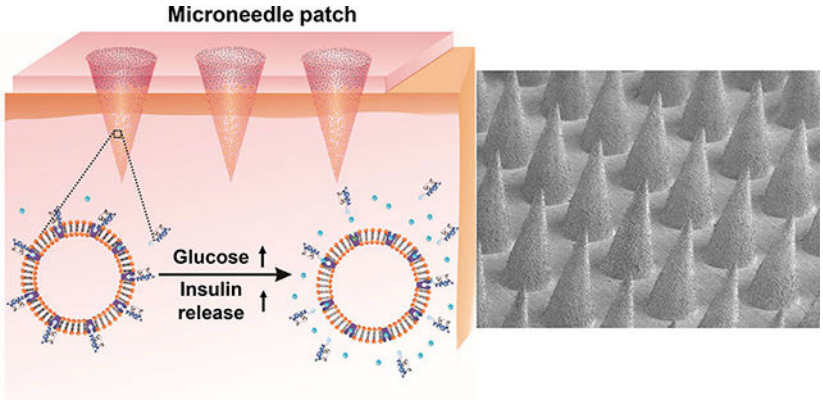

Keywords

drug delivery; glucose transporter; microneedles; diabetes; glucose-responsive

INTRODUCTION

Diabetes mellitus, one chronic disease characterized by the loss of the ability to regulate blood glucose (BG) levels within a normal range, has affected 537 million people worldwide in 2021, and this number is estimated to be 783 million by 2045.[1,2] Insulin, which can help cells translate glucose to energy, is essential for people with type 1 and advanced type 2 diabetes to achieve normoglycemia and reduce complications.[3,4] However, traditional administration of insulin usually fails to match the physiological insulin released by β-cells, which can intelligently secrete suitable amounts of insulin *via* metabolism to glucose transport.[5,6] Failure of glucose control usually can lead to subsequent consequences, including blindness, limb amputation, cardiovascular disease, and kidney failure.[7] In addition, an excess level of insulin can increase the risk of hypoglycemia, which can result in behavioral and cognitive disturbance, coma, brain damage, seizure, or even death.[8] Thus, it is urgent to develop an intelligent glucose-responsive delivery system that can mimic β-cells to "secrete" desirable amounts of insulin to regulate the BG level and improve the quality of life for people with diabetes.[6,9,10]

To achieve this objective, the closed-loop systems that integrate a continued glucose-monitoring sensor and an insulin injection pump have been developed.[1,6,11] However, these systems still have many challenges, including sensor reliability, algorithm accuracy, and biofouling.[6] On the other hand, synthetic material-based glucose-responsive

systems have attracted wide attentions as an alternative strategy over the past few decades.[1,6,9,10,12–16] These systems typically include one of three different glucose-sensing moieties: glucose-binding protein (GBP),[17,18] glucose oxidase (GOx),[12,13,19–22] or phenylboronic acid (PBA).[23–27] Various formulations, including scaffolds, microgels, self-assembled, or emulsion-based nanoparticles, have been exploited to respond to high BG levels and release desirable amounts of insulin by swelling, shrinking degradation, or dissociation.[12,13,19,23,28,29] Despite these promising results, such systems still remain challenging due to concerns, including the long-term toxicity, immunological responses, and stability of these synthetic systems in the physiological environment.

Herein, we report a glucose-responsive insulin delivery system based on the glucose transporter (GLUT) molecules that play an important role in transporting glucose, including glucose transporter 1 (GLUT1), the dominant glucose transporter found in human red blood cells (RBCs), and glucose transporter 4 (GLUT4), the main glucose transporter on mouse RBCs.[30–33] As shown in Figure 1, glucosamine-modified insulin (Glu-Insulin) can successfully bind to the nanovesicles derived from GLUT-expressed RBC membranes *via* a specific GLUT–glucosamine interaction.[34,35] Of note, the interaction between Glu-Insulin and GLUT is reversible, and bound Glu-Insulin can be released quickly in high concentrations of glucose, owing to the displaced interaction between free glucose and GLUT. To achieve ease of administration, RBC vesicles bound with Glu-Insulin (RBC-Insulin vesicles) were loaded into the tips of a microneedle (MN) array patch made from cross-linked hyaluronic acid (HA) for glucose-responsive insulin release. Considering the limited amount of Glu-Insulin bound to RBC vesicles owing to the one-to-one interaction of glucosamine and GLUT, additional Glu-Insulin, which serves as “stored insulin”, is loaded above the RBC-Insulin vesicles. Thus, when exposed to interstitial fluid with high glucose concentrations, Glu-Insulin can be quickly released from RBC-Insulin vesicles in MNs after transcutaneous administration. Presumably, Glu-Insulin loaded in the upper layer is expected to further bind to GLUT expressed on RBC vesicles, similar to a “recharge” process for further glucose-responsive release.

Moreover, this “GLUT-based glucose-responsive insulin release” strategy can be extended by anchoring GLUT1 purified from *E. coli Rosetta* (*DE3*) pLysS cells that express GLUT after transformation with pET28a-rGLUT1 into liposome membranes, forming liposomes (GLUT1). Similar to RBC vesicles, Glu-Insulin can bind to liposomes (GLUT1) and be quickly released from liposomes (GLUT1) in high concentrations of glucose. Similarly, liposome (GLUT1) nanoparticles bound with Glu-Insulin (liposome (GLUT1)-insulin) loaded into MNs together with additional Glu-Insulin in the upper layer can regulate BG levels and avoid hypoglycemia in streptozotocin (STZ)-induced type 1 diabetic mice.

RESULTS AND DISCUSSION

RBC cell membrane vesicles from adult mice containing GLUT4 were prepared using a serial extrusion of vesicles through polycarbonate membrane filters with pore sizes of 0.8 and 0.22 μm (Figure 1).[36] Transmission electron microscopy (TEM) imaging revealed the formation of RBC vesicles, which exhibited a uniform spherical shape with a diameter about 200 nm (Figure 2a), as further verified by the dynamic light scattering (DLS) (Figure

2b). Sodium dodecyl sulfate–polyacrylamide gel electrophoresis (SDS–PAGE) together with Western blot analysis was carried out to verify the presence of GLUTs on RBC vesicles (Figure 2c). The presence of GLUTs on RBC vesicles was further verified by confocal imaging after staining with rhodamine B-labeled anti-GLUT4 antibodies (Figure S1). Glucosamine was conjugated to insulin *via* a bifunctional NHS-maleimide linker (*i.e.*, sulfosuccinimidyl-4-(*N*-maleimidomethyl)-cyclohexane-1-carboxylate), forming Glu-Insulin, which was verified by matrix-assisted laser desorption/ionization mass spectrometry (MALDI-MS) (Figure S2). Then, Glu-Insulin was bound to RBC vesicles through the specific GLUT–glucosamine interaction, which was observed through the confocal imaging (Figure 2d). Importantly, the binding of Glu-Insulin to RBC vesicles could be competitively replaced by D-glucose. As shown in Figure 2d, nearly no insulin signals could be detected after RBC-insulin vesicles were incubated in a 400 mg/dL glucose solution for over 2 hours, indicating the rapid release of Glu-Insulin under hyperglycemic conditions. The insulin loading content of RBC-Insulin vesicles was measured to be 0.5 wt % by the enzyme-linked immunosorbent assay (ELISA).

To evaluate the glucose-responsive release of insulin, RBC-Insulin vesicles were dispersed in the phosphate buffered saline (PBS) solutions with different glucose concentrations, including a control level (0 mg/dL), a normoglycemic level (100 mg/dL), and a typical hyperglycemic level (400 mg/dL). The amount of released Glu-Insulin from RBC-Insulin vesicles was measured by ELISA. Compared to the control or normoglycemic condition (0 or 100 mg/dL glucose), the release of Glu-Insulin significantly increased in the hyperglycemic condition with a glucose concentration of 400 mg/dL (Figure 2e). Furthermore, the release of Glu-Insulin from RBC-Insulin vesicles could be steadily promoted when the concentration of glucose was gradually increased from 0 to 400 mg/dL (Figure 2f). Taken together, these results suggest the potential of the glucose-responsive release of insulin from the RBC-Insulin vesicles *in vivo*.

To realize painless and convenient administration, RBC-Insulin vesicles were loaded in the cross-linked MN-array patch. For the preparation of MNs, a methacrylated HA (m-HA) polymer solution containing RBC-Insulin vesicles was first loaded in the tips of a mold through centrifugation. Then, m-HA polymer solution containing free Glu-Insulin, which served as the “stored insulin”, was loaded above RBC-Insulin vesicles. The prepared MNs were arranged in a 15 × 15 array, and each needle exhibited a conical shape with a diameter of 10 μm for the tip and 300 μm for the base, together with a height about 600 μm (Figure 3a,b). The fluorescence image exhibited a uniform distribution of fluorescein isothiocyanate (FITC)-labeled Glu-Insulin inside the MNs (Figure 3c). The mechanical strength of the cross-linked MNs was measured to be 0.55 N per needle, which was higher than the required minimum strength of 0.1 N to pierce the skin,[37] indicating a sufficient strength of the cross-linked MNs to penetrate into the skin (Figure 3d). The effective penetration of the obtained MNs into the mouse skin was further demonstrated by the trypan blue spots on the skin that were related to the insertion sites of MNs (Figure 3e), which was further confirmed by the hematoxylin and eosin (H&E) staining (Figure 3f). In addition, the wound caused by MNs could heal rapidly within 24 hours (Figure S5).

We then investigated the therapeutic efficacy of MNs loaded with RBC-Insulin vesicles for hyperglycemia treatment in an *STZ*-induced type 1 diabetic mouse model. These diabetic mice were divided into three groups: application of the blank MN patch (Blank MN); subcutaneous injection of free human recombinant insulin (Free insulin); application of the MN patch loaded with RBC-Insulin vesicles and free Glu-Insulin (RBC-insulin-MN) (insulin dose for MN-based treatment: 10 mg/kg). The BG levels of mice after different treatments were closely monitored. As exhibited in Figure 3g, the BG levels of mice treated with RBC-insulin-MN showed a rapid decrease in the first 1 hour and were maintained around 200 mg/dL for up to 5 hours without obvious hypoglycemia, which is longer compared to the subcutaneous administration of free recombinant insulin. This was contributed to the effective glucose-responsive insulin release from the MNs.

To further investigate the *in vivo* glucose-responsive insulin release, intraperitoneal glucose tolerance tests (IPGTTs)[22,26] were carried out 1 hour after treatment with RBC-insulin-MN. As shown in Figure 3h, the BG levels of the healthy mice in the control group showed a quick increase and recovered to normal levels in 1.5 hours. In diabetic mice, the BG levels of mice treated with RBC-insulin-MN showed a delayed increase and declined to the normoglycemic state in 1 hour. In contrast, the BG levels of mice treated with free insulin exhibited a continuous increase to the hyperglycemia state within 1 hour. Moreover, the quantitative glucose response further indicated the enhanced responsiveness of RBC-insulin-MN to IPGTT compared to the free treatment of insulin (Figure 3i). Furthermore, the concentration of insulin in the plasma was also measured by ELISA after IPGTT (Figure 3j). Interestingly, the insulin concentration in the serum followed closely with the fluctuation of BG levels.

To investigate the potential of RBC-insulin-MN to induce hypoglycemia *in vivo*, healthy mice were treated with blank MN, free insulin, or RBC-insulin-MN. Compared to mice treated with free insulin, the BG levels of mice treated with RBC-insulin-MN showed a slight reduction, indicating a reduced risk of hypoglycemia with RBC-insulin-MN treatment (Figure 3k). The corresponding hypoglycemia index calculated by the difference in the initial and nadir BG levels divided by the time further verified that RBC-insulin-MN showed a reduced hypoglycemia index (Figure 3l).

In addition to the RBC vesicles, GLUT1 purified from *Escherichia coli* Rosetta (DE3) pLysS cells, which was verified by SDS–PAGE analysis (Figure S3), could be anchored in the membrane of liposomes for the glucose-responsive insulin release, which exhibited a higher concentration of GLUT1 in comparison with RBC vesicles. Liposomes anchored with GLUT1 were fabricated through the freeze–thaw sonication method according to a previous study[38] (Figure 4a). The obtained liposome with GLUT1 nanoparticles exhibited a consistent spherical shape with a diameter about 100 nm, as shown in the TEM image and DLS (Figure 4b,c). The presence of GLUT1 on the liposome membrane was verified by Western blotting and confocal imaging (Figure 4d,e). The loading efficiency of GLUT1 on the liposome was measured to be 80% *via* GLUT1 ELISA kits. Afterward, Glu-Insulin was bound to liposome (GLUT1) nanoparticles, forming liposome (GLUT1)-insulin through the specific interaction between glucosamine and GLUT1, which was further validated by confocal imaging (Figure S4). The loading capacity of Glu-Insulin on liposomes was

measured to be 1 wt % *via* the insulin ELISA kits. As expected, liposome(GLUT1)-insulin also exhibited a quick release of insulin in a hyperglycemic solution with a glucose concentration of 400 mg/dL (Figure S4 and Figure 5a).

Similar to the RBC-Insulin vesicles, liposome (GLUT1)-insulin was loaded in a cross-linked MN-array patch for hyperglycemia treatment in an STZ-induced type 1 diabetic mouse model. Compared to free insulin, liposome(GLUT1)-insulin-MN could maintain the BG levels of mice for a significantly longer time and reduce the risk of hypoglycemia (Figure 5b–d). The IPGTT was also carried out 1 h postadministration of free insulin or liposome (GLUT1)-insulin-MN. As shown, the liposome (GLUT1)-insulin-MN-treated mice exhibited obviously improved glucose responsiveness to the glucose challenge (Figure 5e,f).

These results, as well as prior findings,[14,39] support the idea of glucose-responsive insulin delivery from a MN patch. The minimally invasive nature of the MN patch that allows for simple self-administration is ideally suited for this application. Current closed-loop systems involving subcutaneous glucose sensors and continuous insulin pumps that are modulated by a feedback-control processor are complex, costly, and cumbersome to use.[40] Their performance is constrained by time lags inherent in the system, which result in difficulty to adjust insulin delivery rates in response to physiological changes like exercise or eating without user input. In contrast, pancreas transplants suffer from limited donor tissue supply and immune rejection issues,[41] while bioartifical pancreas approaches involving encapsulated cells have had limited lifetime *in vivo*.[42] Synthetic insulin-releasing systems, some of which use glucose-responsive chemistry like in this study, require administration by injection or implantation and, in the event of burst release or other dangerous situations, cannot be easily removed from the body.[43]

Glucose-responsive insulin delivery from a MN patch is able to capture the advantages of an indwelling delivery system without the complexity of keeping cells alive and functional or otherwise needing longevity of action. Because the MN patch is inexpensive to manufacture and simple to self-administer,[44] patients can frequently apply a fresh patch (or remove the patch if needed), thereby reducing risks of biofouling, incorrect dosing, or other failures. In this way, a MN patch can simplify and potentially improve glucose management compared to current closed-loop insulin delivery systems and make the convenience and efficacy of closed-loop therapy more broadly available to patients with type 1 as well as type 2 diabetes.

CONCLUSION

In conclusion, a strategy based on RBC vesicles containing GLUT bound with glucosamine-modified insulin was developed for effective glucose-responsive insulin delivery. Under hyperglycemic conditions, Glu-Insulin could be quickly released owing to the competitive binding between Glu-Insulin and glucose. The RBC-Insulin vesicles together with free Glu-Insulin that serves as the “stored insulin” could be integrated with a MN-array patch for convenient and painless delivery, achieving effective regulation of BG levels in mice with STZ-induced type 1 diabetes. This strategy can be further extended to liposomes anchored with GLUT for effective glucose-responsive insulin delivery *via* MN in a noninvasive manner.

MATERIALS AND METHODS

Materials.

All chemicals unless otherwise specified were obtained from Sigma–Aldrich. The lipid dipalmitoyl-*sn*-glycero-3-phosphocholine (DPPC) was purchased from Avanti Polar Lipids. 1,2-Distearoyl-*sn*-glycero-3-phosphoethanolamine *N*-[methoxy(polyethylene glycol)-5000] (DSPE-PEG) was purchased from Laysan Bio Inc. Human recombinant insulin (Zn salt, 27.5 IU/mg) was obtained from Life Technology.

Preparation of Insulin-Loaded RBC Vesicles.

RBCs were isolated from whole blood that was collected from C57BL/6 mice and washed with cold PBS (300 mOsm, pH = 8.0) three times to remove glucose. Then, RBCs were resuspended in water containing 0.2 mM EDTA for 5 min to induce RBC membrane rupture. The RBC suspension was dispersed in PBS and centrifuged at 148,000 rpm for 5 min at 4 °C to obtain the precipitate. The above procedures were repeated until the supernatant was colorless. The RBC membrane was resuspended in homogenization medium (HM) buffer (0.25 M sucrose, 1 mM EDTA, 20 mM HEPES-NaOH, pH 7.4, and protease inhibitor cocktail) and was sonicated until the solution was transparent. To prepare the RBC vesicles, the RBC membrane solution was extruded 10 times through 0.8 μm filters and was then extruded through 0.22 μm filters for an additional 10 times. Subsequently, Glu-Insulin prepared according to a previous study[45] was incubated with RBC vesicles under gentle stirring overnight at 4 °C to obtain RBC-insulin vesicles. RBC-insulin vesicles were washed by centrifugation using PBS (cold, pH 8) to remove unloaded Glu-Insulin and were then stored at 4 °C for further use.

Preparation of Insulin-Bound Liposomes Containing GLUT1.

Liposomes were prepared by dissolving DSPE-PEG, cholesterol, and DPPC at a molar ratio of 0.5:4:6 in chloroform. The solution was evaporated by rotary evaporation to yield a lipid film. Then, 1 mL of PBS was added, and this mixture was sonicated at 60 °C to obtain a transparent suspension. Afterward, the solution was extruded through a 200 nm filter 20 times. Then, GLUT1 (method of the expression and purification described in the Supporting Information) was reestablished on the liposome membrane according to a previous study.[46] Briefly, 0.5 mg of GLUT1 was mixed with 5 mg of liposome dispersed in PBS, which was then frozen in liquid nitrogen and rehydrated in 60 °C bath for five repeated freezing and thawing cycles. Then, Glu-Insulin was incubated with liposomes (GLUT1) under gentle stirring overnight at 4 °C to obtain Glu-Insulin-loaded liposomes (GLUT1). Liposome (GLUT1)-insulin was obtained by centrifugation using PBS (cold, pH 8) to remove unloaded Glu-Insulin and stored at 4 °C until use.

In Vitro Release Studies.

To study the glucose-responsive insulin release behavior, RBC-insulin vesicles or liposome (GLUT1)-insulin were dispersed in solutions with different glucose concentrations (0, 100, or 400 mg/dL). At different time points, the solutions were centrifuged, and the released insulin was measured by ELISA.

Fabrication of RBC-Insulin Vesicles or Liposome (GLUT1)-Insulin Loaded MNs.

All of the MNs used in this work were fabricated with uniform silicone molds purchased from Blueacre Technology Ltd. Each MN had a base with a diameter about 300 μm, which tapered to a height of 600 μm tip with the diameter about 10 μm. These needles were arranged in a 15 × 15 array. To fabricate RBC-insulin vesicles or liposome(GLUT1)-insulin loaded MNs, 150 μL of m-HA (2 wt %) solution containing RBC-insulin vesicles or liposome (GLUT1)-insulin, *N,N'*-methylenebis(acrylamide) (MBA, w/v = 2%), and a photoinitiator (Irgacure 2959, w/v = 0.5%) were deposited onto each MN mold, which was then kept in a reduced vacuum (600 mmHg) for 30 min. Afterward, molds were centrifuged at 1000 rpm for 20 min using a Hettich Niversal 32R centrifuge to compact the nanoparticles into the MN cavities. Afterward, 0.4 mL of m-HA (4 wt %) solution containing Glu-Insulin (0.4 wt %), *N,N'*-methylenebis(acrylamide) (MBA, w/v = 2%), and a photoinitiator (Irgacure 2959, w/v = 0.5%) were added to each prepared mold in a vacuum desiccator and dried for 2 hours. Finally, 1 mL of HA (4 wt %) was added to each prepared mold in a vacuum desiccator and dried in a vacuum desiccator overnight. After the completion of desiccation, the MNs were carefully peeled off from the molds and polymerized under UV light irradiation. The fluorescent MNs were prepared with FITC-labeled insulin. The morphology of the MNs was characterized by an FEI Verios 460 L field emission scanning electron microscope (FESEM). Fluorescence images were obtained using an Olympus IX70 multiparameter fluorescence microscope.

In Vivo Studies Using STZ-Induced Type 1 Diabetic Mice.

The *in vivo* efficiency of MN patches for diabetes therapy was investigated in STZ-induced male C57BL/6 diabetic mice (6–10 weeks) purchased from Jackson Laboratory (USA). The protocol of the animal study was approved by the Institutional Animal Care and Use Committee at North Carolina State University and the University of North Carolina at Chapel Hill. The plasma glucose was detected *via* ~3 μL blood samples obtained from the tail vein of each mouse using a Clarity GL2Plus glucose meter (Clarity Diagnostics). Mouse glucose levels were monitored for 2 days before the experiment. Five mice were selected for each group and were treated with the MN patch or native insulin. The plasma glucose levels were measured over time. To detect the concentration of insulin in the plasma, blood samples were collected from each mouse at different time points. The serum was isolated, and the insulin concentration was measured by the Human Insulin ELISA kit according to the manufacturer's protocol.

Statistical Analysis.

All results are presented as the mean ± s.e.m. Statistical analysis was performed utilizing Student's *t* test or one-way analysis of variance (ANOVA). The threshold for statistical significance was $P < 0.05$.

Supplementary Material

Refer to Web version on PubMed Central for supplementary material.

ACKNOWLEDGMENTS

This work was supported by grants from the National Institutes of Health (R01DK112939 and R01CA234343-01A1) and American Diabetes Association (grant no. 1-15-ACE-21). This work was performed in part at the Analytical Instrumentation Facility (AIF) at North Carolina State University, which is supported by the State of North Carolina and the National Science Foundation (grant no.1542015). The AIF is a member of the North Carolina Research Triangle Nanotechnology Network (RTNN), a site in the National Nanotechnology Coordinated Infrastructure (NNCI).

REFERENCES

(1). Mo R; Jiang T; Di J; Tai W; Gu Z Emerging micro-and nanotechnology based synthetic approaches for insulin delivery. Chem. Soc. Rev. 2014, 43 (10), 3595–3629. [PubMed: 24626293]

(2). Moheman A; Alam MS; Mohammad A Recent trends in electrospinning of polymer nanofibers and their applications in ultra thin layer chromatography. Adv. Colloid Interface Sci. 2016, 229, 1–24. [PubMed: 26792019]

(3). Pickup J; Keen H Continuous subcutaneous insulin infusion at 25 years: evidence base for the expanding use of insulin pump therapy in type 1 diabetes. Diabetes care 2002, 25 (3), 593–598. [PubMed: 11874953]

(4). Raskin P; Allen E; Hollander P; Lewin A; Gabbay RA; Hu P; Bode B; Garber A Initiating insulin therapy in type 2 diabetes: a comparison of biphasic and basal insulin analogs. Diabetes care 2005, 28 (2), 260–265. [PubMed: 15677776]

(5). Wu Q; Wang L; Yu H; Wang J; Chen Z Organization of glucose-responsive systems and their properties. Chem. Rev. 2011, 111 (12), 7855–7875. [PubMed: 21902252]

(6). Veiseh O; Tang BC; Whitehead KA; Anderson DG; Langer R Managing diabetes with nanomedicine: challenges and opportunities. Nat. Rev. Drug Discovery 2015, 14 (1), 45–57. [PubMed: 25430866]

(7). Nathan DM Long-term complications of diabetes mellitus. New Engl. J. Med. 1993, 328 (23), 1676–1685. [PubMed: 8487827]

(8). Ohkubo Y; Kishikawa H; Araki E; Miyata T; Isami S; Motoyoshi S; Kojima Y; Furuyoshi N; Shichiri M Intensive insulin therapy prevents the progression of diabetic microvascular complications in Japanese patients with non-insulin-dependent diabetes mellitus: a randomized prospective 6-year study. Diabetes Res. Clin. Pr. 1995, 28 (2), 103–117.

(9). Gilroy CA; Luginbuhl KM; Chilkoti A Controlled release of biologics for the treatment of type 2 diabetes. J. Controlled Release 2016, 240, 151–164.

(10). Bratlie KM; York RL; Invernale MA; Langer R; Anderson DG Materials for diabetes therapeutics. Adv. Healthc. Mater. 2012, 1 (3), 267–284. [PubMed: 23184741]

(11). Wang Z; Wang J; Kahkoska AR; Buse JB; Gu Z Developing insulin delivery devices with glucose responsiveness. Trends Pharmacol. Sci. 2021, 42 (1), 31–44. [PubMed: 33250274]

(12). Gu Z; Dang TT; Ma M; Tang BC; Cheng H; Jiang S; Dong Y; Zhang Y; Anderson DG Glucose-responsive microgels integrated with enzyme nanocapsules for closed-loop insulin delivery. ACS Nano 2013, 7 (8), 6758–6766. [PubMed: 23834678]

(13). Gu Z; Aimetti AA; Wang Q; Dang TT; Zhang Y; Veiseh O; Cheng H; Langer RS; Anderson DG Injectable nano-network for glucose-mediated insulin delivery. ACS Nano 2013, 7 (5), 4194–4201. [PubMed: 23638642]

(14). Yu J; Wang J; Zhang Y; Chen G; Mao W; Ye Y; Kahkoska AR; Buse JB; Langer R; Gu Z Glucose-responsive insulin patch for the regulation of blood glucose in mice and minipigs. Nat. Biomed. Eng. 2020, 4 (5), 499–506. [PubMed: 32015407]

(15). Wang Z; Wang J; Li H; Yu J; Chen G; Kahkoska AR; Wu V; Zeng Y; Wen D; Miedema JR; et al. Dual self-regulated delivery of insulin and glucagon by a hybrid patch. Proc. Natl. Acad. Sci. U. S. A. 2020, 117 (47), 29512–29517. [PubMed: 33177238]

(16). Luo F-Q; Chen G; Xu W; Zhou D; Li J-X; Huang Y-C; Lin R; Gu Z; Du J-Z Microneedle-array patch with pH-sensitive formulation for glucose-responsive insulin delivery. Nano Research 2021, 14 (8), 2689–2696.

(17). Wang C; Ye Y; Sun W; Yu J; Wang J; Lawrence DS; Buse JB; Gu Z Red Blood Cells for Glucose-Responsive Insulin Delivery. Adv. Mater. 2017, 29 (18), 1.

(18). Joel S; Turner KB; Daunert S Glucose recognition proteins for glucose sensing at physiological concentrations and temperatures. ACS Chem. Biol. 2014, 9 (7), 1595–1602. [PubMed: 24841549]

(19). Hu X; Yu J; Qian C; Lu Y; Kahkoska AR; Xie Z; Jing X; Buse JB; Gu Z H2O2-responsive vesicles integrated with transcutaneous patches for glucose-mediated insulin delivery. ACS Nano 2017, 11 (1), 613–620. [PubMed: 28051306]

(20). Zhang K; Wu XY Modulated insulin permeation across a glucose-sensitive polymeric composite membrane. J. Controlled Release 2002, 80 (1–3), 169–178.

(21). Tai W; Mo R; Di J; Subramanian V; Gu X; Buse JB; Gu Z Bio-inspired synthetic nanovesicles for glucose-responsive release of insulin. Biomacromolecules 2014, 15 (10), 3495–3502. [PubMed: 25268758]

(22). Yu J; Zhang Y; Ye Y; DiSanto R; Sun W; Ranson D; Ligler FS; Buse JB; Gu Z Microneedle-array patches loaded with hypoxia-sensitive vesicles provide fast glucose-responsive insulin delivery. Proc. Natl. Acad. Sci. U.S.A. 2015, 112 (27), 8260–8265. [PubMed: 26100900]

(23). Kataoka K; Miyazaki H; Bunya M; Okano T; Sakurai Y Totally synthetic polymer gels responding to external glucose concentration: their preparation and application to on- off regulation of insulin release. J. Am. Chem. Soc. 1998, 120 (48), 12694–12695.

(24). Shiino D; Murata Y; Kubo A; Kim YJ; Kataoka K; Koyama Y; Kikuchi A; Yokoyama M; Sakurai Y; Okano T Amine containing phenylboronic acid gel for glucose-responsive insulin release under physiological pH. J. Controlled Release 1995, 37 (3), 269–276.

(25). Matsumoto A; Yoshida R; Kataoka K Glucose-responsive polymer gel bearing phenylborate derivative as a glucose-sensing moiety operating at the physiological pH. Biomacromolecules 2004, 5 (3), 1038–1045. [PubMed: 15132698]

(26). Chou DH-C; Webber MJ; Tang BC; Lin AB; Thapa LS; Deng D; Truong JV; Cortinas AB; Langer R; Anderson DG Glucose-responsive insulin activity by covalent modification with aliphatic phenylboronic acid conjugates. Proc. Natl. Acad. Sci. U. S. A. 2015, 112 (8), 2401–2406. [PubMed: 25675515]

(27). Dong Y; Wang W; Veiseh O; Appel EA; Xue K; Webber MJ; Tang BC; Yang X-W; Weir GC; Langer R; et al. Injectable and glucose-responsive hydrogels based on boronic acid-glucose complexation. Langmuir 2016, 32 (34), 8743–8747. [PubMed: 27455412]

(28). Kim H; Kang YJ; Kang S; Kim KT Monosaccharide-responsive release of insulin from polymersomes of polyboroxole block copolymers at neutral pH. J. Am. Chem. Soc. 2012, 134 (9), 4030–4033. [PubMed: 22339262]

(29). Mi F-L; Wu Y-Y; Lin Y-H; Sonaje K; Ho Y-C; Chen C-T; Juang J-H; Sung H-W Oral delivery of peptide drugs using nanoparticles self-assembled by poly (γ-glutamic acid) and a chitosan derivative functionalized by trimethylation. Bioconjugate Chem. 2008, 19 (6), 1248–1255.

(30). Montel-Hagen A; Blanc L; Boyer-Clavel M; Jacquet C; Vidal M; Sitbon M; Taylor N The Glut1 and Glut4 glucose transporters are differentially expressed during perinatal and postnatal erythropoiesis. Blood 2008, 112 (12), 4729–4738. [PubMed: 18796630]

(31). Montel-Hagen A; Sitbon M; Taylor N Erythroid glucose transporters. Curr. Opin. Hematol. 2009, 16 (3), 165–172. [PubMed: 19346941]

(32). Vrhovac I; Breljak D; Sabolic I Glucose transporters in the mammalian blood cells. Period. Biol. 2014, 116 (2), 131–138.

(33). Mueckler M Facilitative glucose transporters. FEBS J. 1994, 219 (3), 713–725.

(34). Ranganathan D; Thamake S; Tworowska I; Delpassand E Chelator based glucosamine derivative for Ga-68 based diagnostic PET imaging of malignant tumors. J. Nucl. Med. 2014, 55 (supplement 1), 1004.

(35). Uldry M; Ibberson M; Hosokawa M; Thorens B GLUT2 is a high affinity glucosamine transporter. FEBS Lett. 2002, 524 (1–3), 199–203. [PubMed: 12135767]

(36). Fang RH; Hu C-MJ; Luk BT; Gao W; Copp JA; Tai Y; O'Connor DE; Zhang L Cancer cell membrane-coated nanoparticles for anticancer vaccination and drug delivery. Nano Lett. 2014, 14 (4), 2181–2188. [PubMed: 24673373]

(37). Prausnitz MR Microneedles for transdermal drug delivery. Adv. Drug Delivery Rev. 2004, 56 (5), 581–587.

(38). Kasahara M; Hinkle PC Reconstitution of D-glucose transport catalyzed by a protein fraction from human erythrocytes in sonicated liposomes. Proc. Natl. Acad. Sci. U. S. A. 1976, 73 (2), 396–400. [PubMed: 1061142]

(39). Chen G; Yu J; Gu Z Glucose-Responsive Microneedle Patches for Diabetes Treatment. J. Diabetes Sci. Technol. technology 2019, 13 (1), 41–48.

(40). Allen N; Gupta A Current Diabetes Technology: Striving for the Artificial Pancreas. Diagnostics 2019, 9 (1), 31. [PubMed: 30875898]

(41). Lombardo C; Perrone VG; Amorese G; Vistoli F; Baronti W; Marchetti P; Boggi U Update on pancreatic transplantation on the management of diabetes. Minerva Med. 2017, 108 (5), 405–418. [PubMed: 28466634]

(42). Soetedjo AAP; Lee JM; Lau HH; Goh GL; An J; Koh Y; Yeong WY; Teo AKK Tissue engineering and 3D printing of bioartificial pancreas for regenerative medicine in diabetes. Trends Endocrinol. Metab. 2021, 32 (8), 609–622. [PubMed: 34154916]

(43). Wang J; Wang Z; Yu J; Kahkoska AR; Buse JB; Gu Z Glucose-Responsive Insulin and Delivery Systems: Innovation and Translation. Adv. Mater. 2020, 32 (13), 1902004.

(44). Prausnitz MR; Prausnitz JM Engineering Microneedle Patches for Vaccination and Drug Delivery to Skin. Annu. Rev. Chem. Biomol. Eng. 2017, 8, 177–200. [PubMed: 28375775]

(45). Wang C; Ye Y; Sun W; Yu J; Wang J; Lawrence DS; Buse JB; Gu Z Red Blood Cells for Glucose-Responsive Insulin Delivery. Adv. Mater. 2017, 29 (18), 1606617.

(46). Chen Z; Wang J; Sun W; Archibong E; Kahkoska AR; Zhang X; Lu Y; Ligler FS; Buse JB; Gu Z Synthetic beta cells for fusion-mediated dynamic insulin secretion. Nat. Chem. Biol. 2018, 14 (1), 86–93. [PubMed: 29083418]

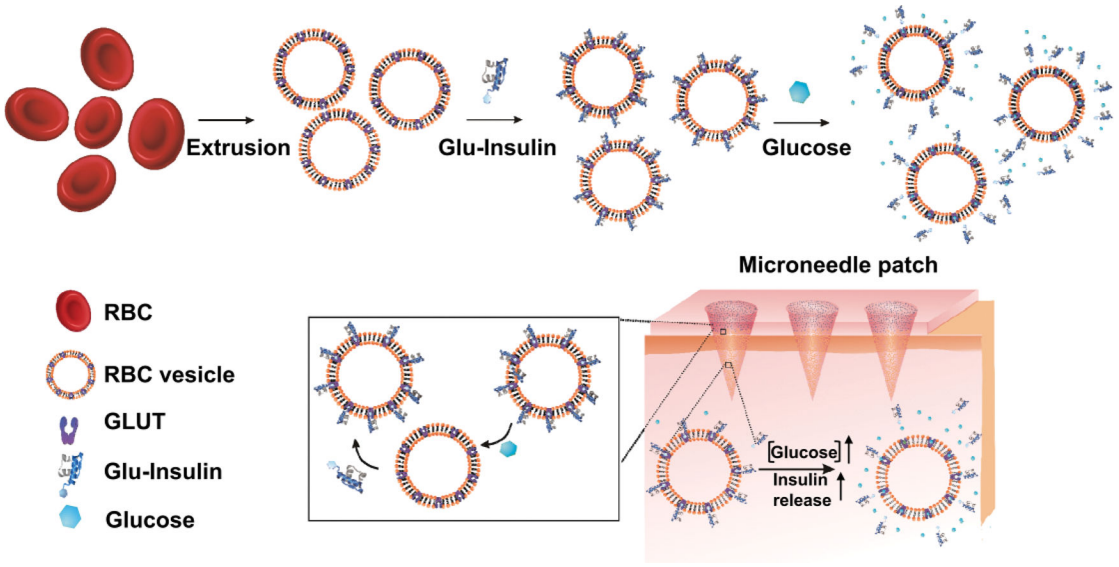

Figure 1.

Schematic showing the glucose-responsive insulin delivery system utilizing a microneedle-array patch encapsulated with red blood cell (RBC) vesicles bound with glucosamine-modified insulin (Glu-Insulin) together with additional free Glu-Insulin. Glu-Insulin can be quickly released under hyperglycemic conditions owing to the competitive interaction between Glu-Insulin and glucose. The additional Glu-Insulin loaded in the upper layer is expected to further bind to GLUT expressed on RBC vesicles, similar to a “recharge” process for further glucose-responsive release.

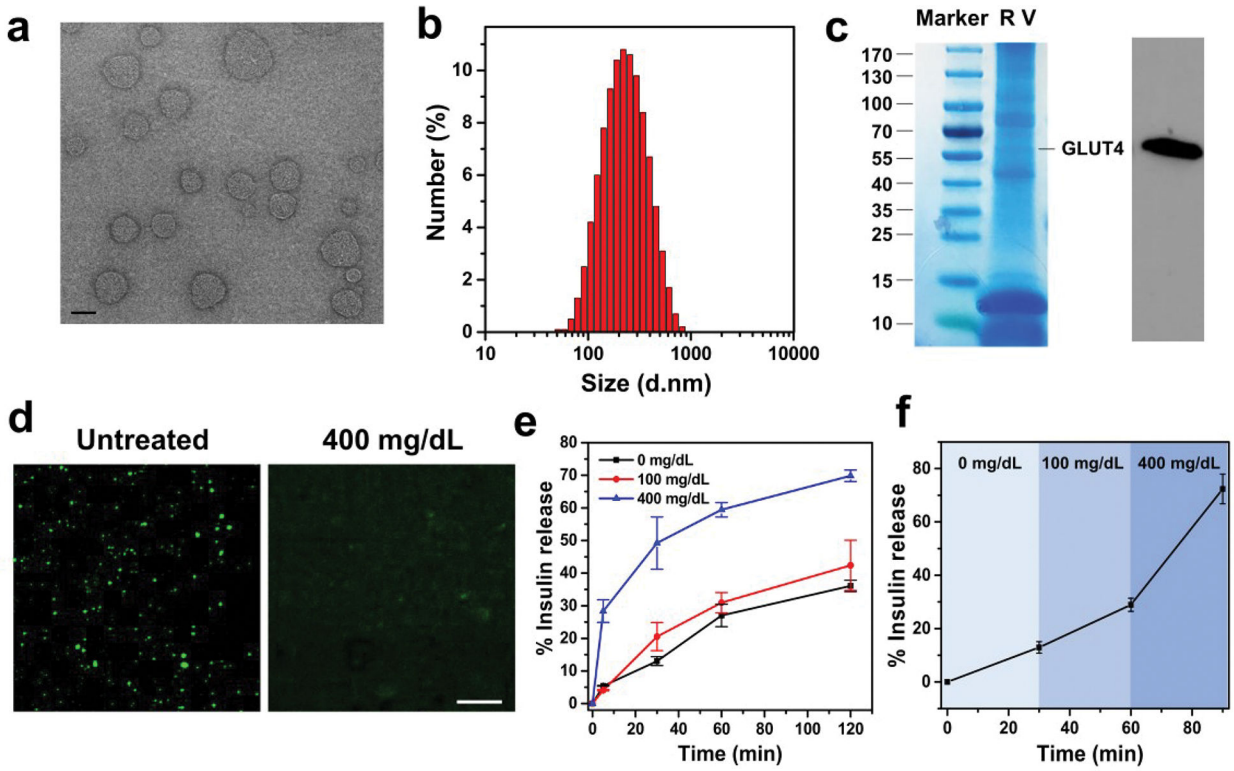

Figure 2.

Characterization of the Glu-Insulin attached RBC vesicles. (a) TEM image showing the size and morphology of RBC vesicles (scale bar: 200 nm). (b) Size-distribution histogram of RBC vesicles measured by DLS. (c) SDS–PAGE and Western blot analysis of the obtained RBC vesicles, indicating the existence of GLUT4 on RBC vesicles. (d) Confocal microscopy images of the Glu-Insulin attached RBC vesicles untreated or treated with 400 mg/dL glucose solution (scale bar: 10 μm). (e) *In vitro* accumulated Glu-Insulin release from the RBC vesicles in solutions with different glucose concentrations. (f) Self-regulated insulin release profile of the RBC vesicles as a function of glucose concentration. The error bars represent the standard error of the mean (s.e.m.) (n = 4). Green color indicated FITC-labeled insulin.

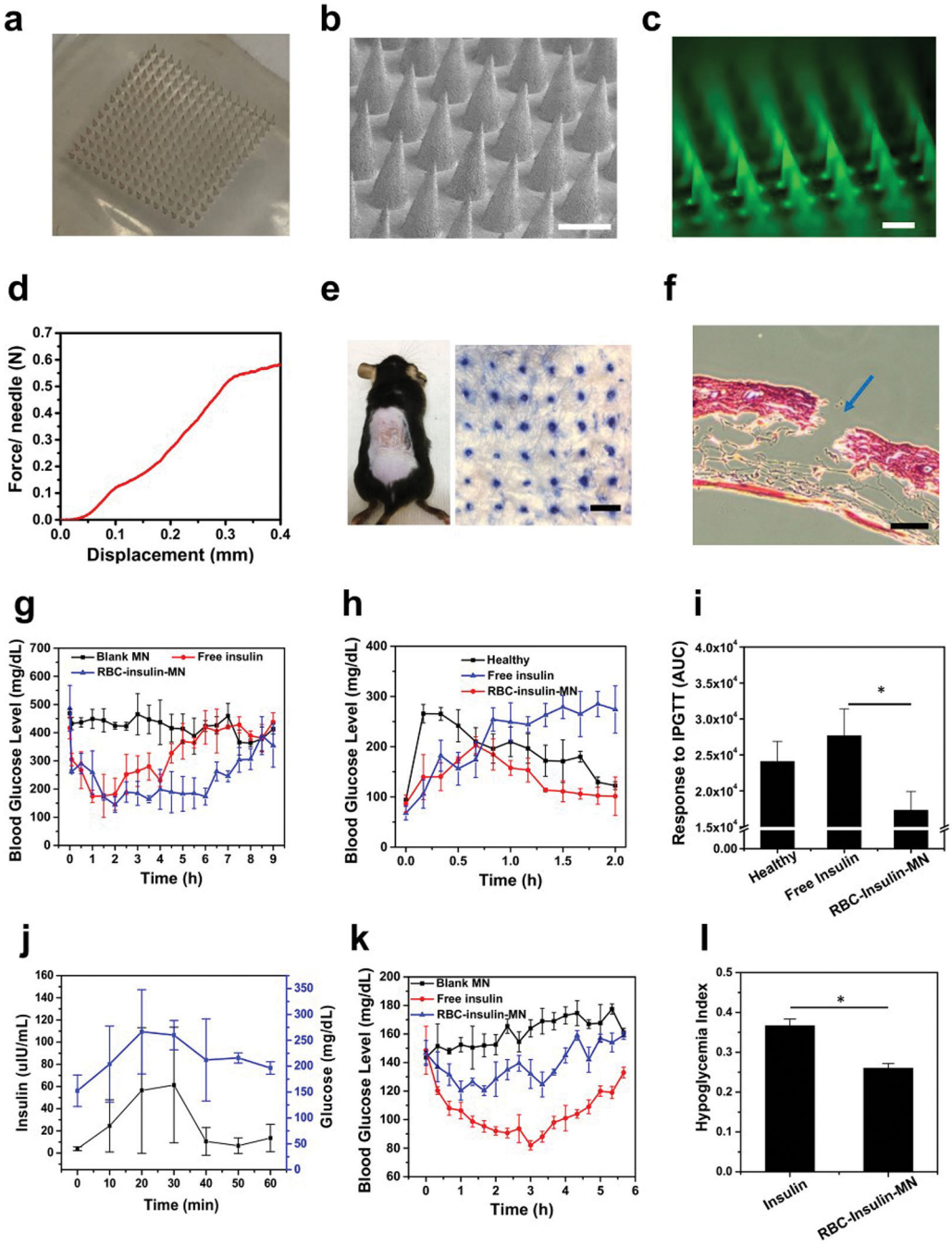

Figure 3.

In vivo evaluation of RBC vesicle-loaded MN array patches for the treatment of type 1 diabetes. (a) Photos of the MN array. (b) SEM image of the MN array (scale bar is 400 μm). (c) Fluorescence microscopy image of MNs containing FITC-labeled insulin-attached RBC vesicles (scale bar is 400 μm). (d) Mechanical property of the MN. The failure force for the desired MN was quantitatively measured to be 0.6 N/needle. (e) Mouse dorsum skin was transcutaneously treated with one MN patch, and the image of trypan blue-stained mouse skin showing the penetration of the MN patch into the skin (scale bar is 500 μm).

(f) H&E-stained section of a cross-sectional mouse skin area penetrated by one MN (blue arrow indicates the area penetrated by one MN; scale bar: 500 μm). (g) BG levels in STZ-induced diabetic mice after different treatments. (h) *In vivo* glucose tolerance test in STZ-induced diabetic mice at 1 h post treatment of MN or subcutaneously injected with insulin. Nondiabetic mice were also used as the control. (i) Responsiveness was calculated based on the area under the curve in 120 min. (j) Change in plasma insulin levels and glucose levels after IPGTT. (k) BG levels of healthy mice treated with MN or subcutaneously injected with insulin over time. (l) Quantification of the hypoglycemia index, calculated from the difference between the initial and nadir BG readings divided by the time at which nadir was reached. The error bars represent the standard error of the mean (s.e.m.) ($n = 5$). P value: $^{*}P < 0.05$.

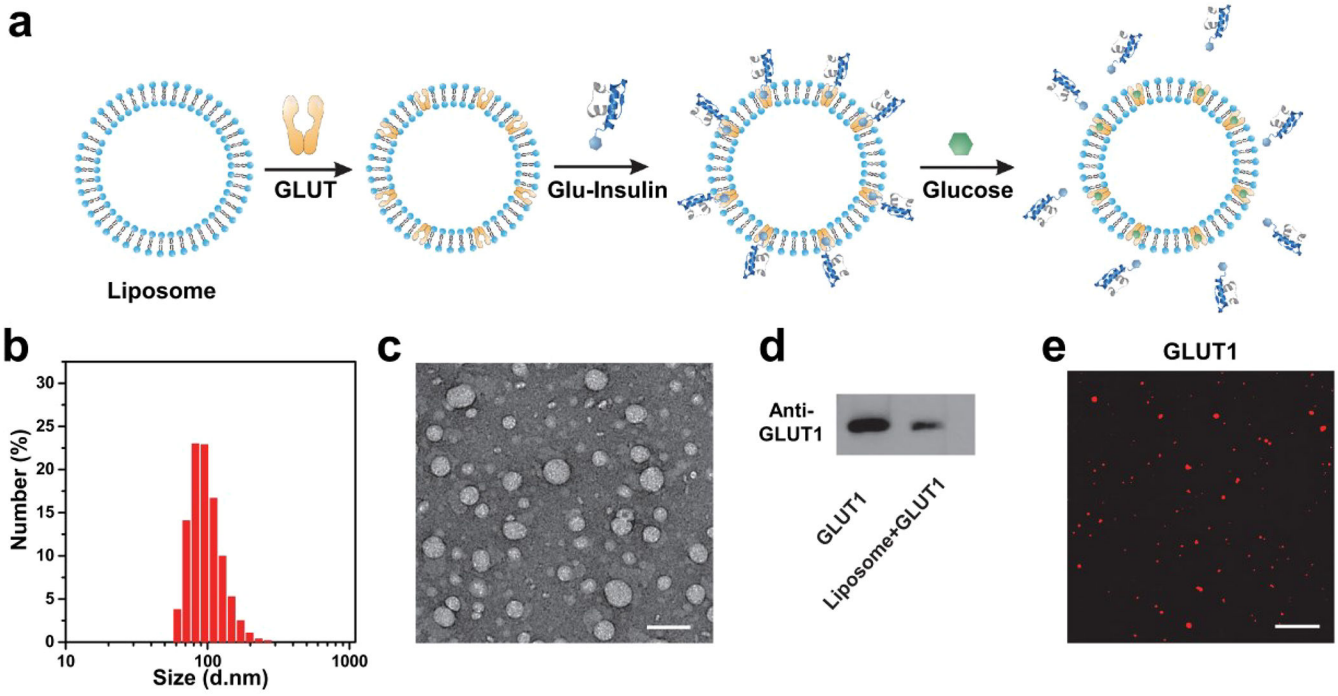

Figure 4.

Preparation of liposomes anchored with GLUT1. (a) Schematic showing the fabrication of liposomes anchored with GLUT. Glu-Insulin can bind to liposome-GLUT1 and be released from liposome-GLUT1 quickly in high concentrations of glucose. (b) Size-distribution histogram of liposome-GLUT1 measured by DLS. (c) TEM image showing the size and morphology of liposome-GLUT1 (scale bar: 200 nm). (d) Western blot analysis of liposome-GLUT1 indicating the presence of GLUT1 in the liposomes. (e) Immunofluorescence imaging of GLUT1 in the liposomes (scale bar: 10 μm).

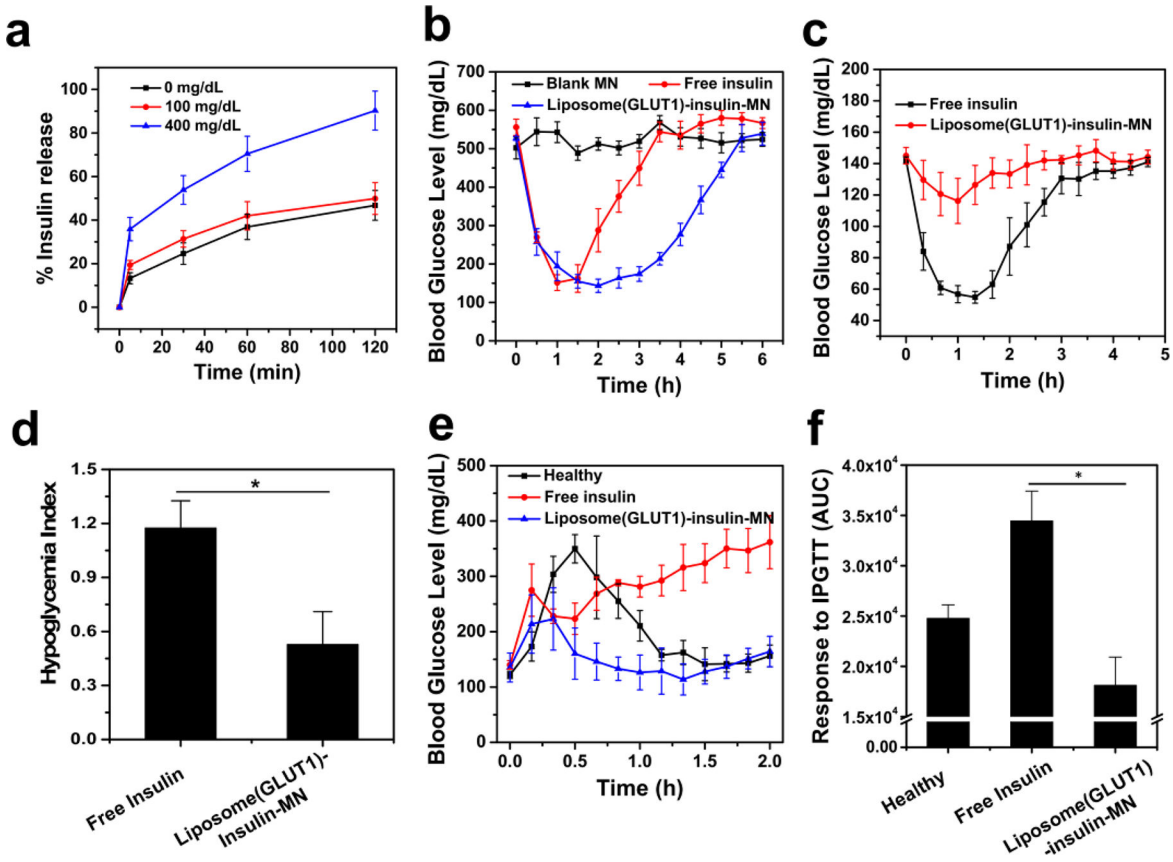

Figure 5.

Glucose-responsive insulin delivery using liposomes anchored with GLUT1. (a) *In vitro* release of Glu-Insulin from liposome-GLUT1 in solutions with different glucose concentrations. (b) BG levels in STZ-induced diabetic mice after different treatments. (c) BG levels of healthy mice treated with MNs loaded with liposome (GLUT1)-insulin or subcutaneously injected with insulin over time. (d) Quantification of the hypoglycemia index, calculated from the difference between the initial and nadir BG readings divided by the time at which nadir was reached. (e) *In vivo* glucose tolerance test in STZ-induced diabetic mice at 1 hour post treatment of MN or subcutaneously injected with insulin. Nondiabetic mice were also used as the control. (f) Responsiveness was calculated based on the area under the curve in 120 min. The error bars represent the standard error of the mean (s.e.m.) ($n = 5$). P value: $^*P < 0.05$.